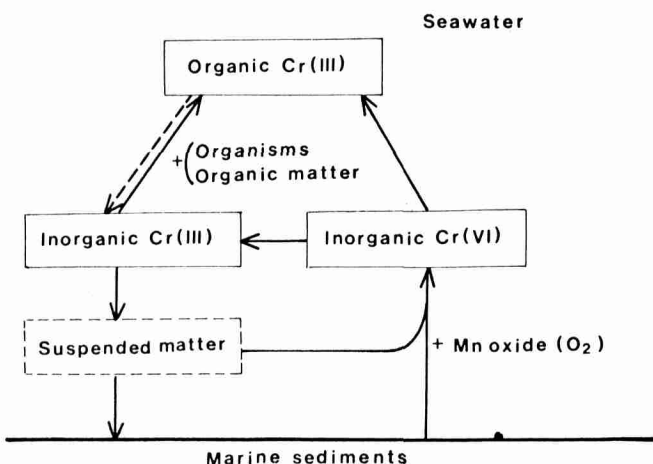


Table 1 Literature data on the chromium contents in seawater

Ref.	Locations	Concentration of chromium ($\mu\text{g l}^{-1}$)	Ratio of Cr(VI)/Cr(III)
1	British coastal	Cr(III) 0.46 Cr(VI) 0	Cr(III) only
2, 3	Ligurian Sea	Cr(III) 0.02–0.25 Cr(VI) 0.05–0.36	Cr(VI) > Cr(III)
4	Pacific Ocean	Cr(III) 0.13–0.90 Cr(VI) 0.07–0.27	Cr(VI) < Cr(III)
5	Equatorial region of Pacific Ocean	Cr(III) 0.24–0.52 Cr(VI) 0.03–0.11	Cr(VI) < Cr(III)
6	Northern north Pacific Ocean	Total Cr 0.16–0.95 Cr(VI) 5–70%	Cr(VI) < Cr(III)
7	North-east region of Pacific Ocean	Cr(III) 0.005 Cr(VI) 0.15	Cr(VI) >> Cr(III)

3.6×10^{-10} M ($0.07 \mu\text{g l}^{-1}$) in the Pacific Ocean and 4.2×10^{-10} M ($0.08 \mu\text{g l}^{-1}$) in the Japan Sea. Figures 1 and 2 show that the vertical distribution of Cr(VI) differs between the two Seas. In the Pacific Ocean there is a remarkable increase at a depth of 1,000 m and below while in the Japan Sea there is a decrease. The ratio of Cr(VI) to inorganic Cr(III) averages 2.7 in the Pacific Ocean while in the Japan Sea it averages 1.8. This difference cannot be explained by thermodynamical equilibrium and application of the oceanographical data, such as pH and dissolved oxygen¹⁰, because the two seas are completely oxygenated. Hence we propose a model for the circulation of chromium in seawater as shown in Fig. 3. This model was supported by an experiment based on the geochemical fact that in manganese nodules the chromium content is extremely low compared with that in the marine sediments composed of clay minerals¹¹. Thus, when the seawater solution containing 10^{-5} M of Cr(III) was bubbled with air for >300 h no hexavalent chromium was detected. However, when about 50 mg l^{-1} of powdered manganese oxide (such as synthesized manganite and manganese nodules) were added, 10% of Cr(III) was oxidized within 100 h. Organic complexes of Cr(III) (such as chromic citrate) were not oxidized within 100 h even if excess manganese oxide was present. From this model, the behaviour of chromium in seawater can be explained as follows. When inorganic Cr(III) is adsorbed by suspended particles it is oxidized by the catalytic action of manganese oxide during sedimentation or in the marine sediments. Direct oxidation with dissolved oxygen only is not appreciable. Cr(VI) is reduced by being taken into organisms or by reductive organic matter. When organic species form, oxidation ceases.

Thus we interpret the difference of distribution of Cr(VI) between the two Seas as being due to the fact that the marine sediments contain abundant manganese oxide in the Pacific Ocean because they are oxygenated down to a considerable depth, whereas the sediments in the Japan Sea, except for a thin oxygenated layer at the surface reduce manganese oxide to Mn(II) (ref. 12). Accordingly, Cr(VI) is supplied to the water

**Fig. 3** A model for the circulation of chromium in seawater.

column in the Pacific Ocean, but not to the Japan Sea. In addition, the Cr(VI) supplied from suspended particles does not seriously effect its vertical distribution because their chromium content is very low.

We thank members of the staff of the Ocean Research Institute, University of Tokyo for their cooperation in the collection of samples.

Received 25 September 1980; accepted 24 February 1981.

- Chuecas, L. & Riley, J. P. *Analyt. chim. Acta* **35**, 240–246 (1966).
- Fukai, R. *Nature* **213**, 901 (1967).
- Fukai, R. & Vas, D. *J. oceanogr. Soc. Jap.* **23**, 298–302 (1967).
- Kuwamoto, T. & Murai, S. *Preliminary Rep. Hakuho-maru Cruise KH-68-4*, 72 (Ocean Research Institute, University of Tokyo, 1970).
- Grimaud, D. & Michard, G. *Mar. Chem.* **2**, 229–237 (1974).
- Yamamoto, T., Kadowaki, S. & Carpenter, J. H. *Geochem. J.* **8**, 123–133 (1974).
- Cranston, R. E. & Murray, J. M. *Analyt. Chim. Acta* **99**, 275–282 (1978).
- Fujinaga, T., Kuwamoto, T., Murai, S., Kihara, S. & Nakayama, E. *Nippon Kagaku Zasshi* **92**, 339–344 (1971).
- Fujinaga, T., Kuwamoto, T., Nakayama, E. & Tsurubo, S. *Abstr. Papers ACS/CSJ Chem. Congr. Envir. Chem. No. 100* (Honolulu, Hawaii, 1979).
- Elderfield, H. *Earth planet. Sci. Lett.* **9**, 10–16 (1970).
- Turekian, K. K. *Chemical Oceanography* Vol. 2, 81–125 (Academic, New York, 1955).
- Masuzawa, T. *Abstr. oceanogr. Soc. Jap.*, 148–149 (1978).

Effect of irregular fluctuations in Antarctic precipitation on global sea level

J. Oerlemans

Institute of Meteorology and Oceanography, University of Utrecht, Postbus 80.005, 3508 TA Utrecht, The Netherlands

One of the reasons for the continuing interest in the global sea level is that secular variations may be caused by climatic changes. Such a change could, for example, be an atmospheric warming due to CO₂ accumulation. Changes in the amount of ice in the major ice sheets will be reflected in secular variations of sea level; it has, for example, been suggested that ice-shelf thinning may change the drainage of parts of the Antarctic Ice Sheet¹. Attempts to monitor climatic change by measuring global sea level will, however, be complicated by random fluctuations of the ice volume in the major ice sheets, themselves the consequence of random variations in the ice accumulation rate. Precipitation rates are highly variable, and this also applies to Antarctica², which stores most of the continental ice mass. By means of a simple model for ice flow in the Antarctic, together with proxy data on precipitation variability derived from ice cores, I show that long-term sea-level variations with a standard deviation of roughly 5 cm are to be expected on this account. This 'climatic noise' is comparable in magnitude with many of the secular effects now being sought.

Any changes in the volume of the Antarctic Ice sheet are damped by a mechanism involving several drainage systems³. In these systems ice is discharged to the ocean by horizontal pressure gradients resulting from differences in elevation of the ice surface. If the ice thickness of a drainage system is increased (without changing the mass balance—the yearly gain of ice mass at the surface), the mean pressure gradient from the interior of the drainage system to the ocean will become larger. The subsequent increase in ice-mass discharge will try to restore the original ice thickness. In the following, we will measure the strength of this damping by the relaxation time, t_R , which indicates how fast the system can return to equilibrium.

Once this time scale is known, the effect of random fluctuations in the mass balance on the volume of the Antarctic Ice Sheet can be estimated with a simple stochastic model. A framework for the application of stochastic models to climate problems has been presented by Hasselmann⁴. Here I will use a simple model, consisting of a rate equation for ice thickness with a linear damping term and an additive stochastic term to represent the fluctuations in the ice accumulation rate.

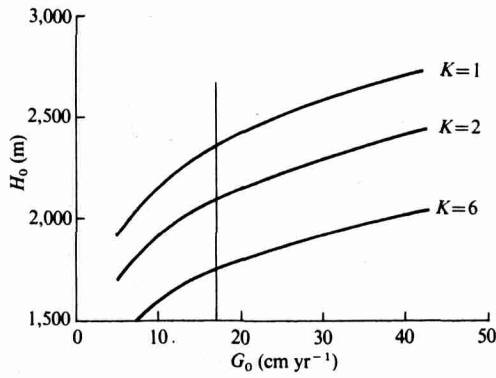


Fig. 1 Steady-state ice thickness H_0 , as a function of the mass balance G_0 , for three values of the flow parameter K ($m^{-3/2} yr^{-1}$). The vertical line indicates the present mass balance over Antarctica.

To obtain a value for t_R , we can turn to a schematic physical description of the dynamics of large ice streams. As proposed by Nye⁵, we use a flow law for the vertically integrated horizontal ice velocity (denoted by u), which should account for both internal deformation and (moderate) basal sliding. It reads

$$u = k\tau_b^m \tag{1}$$

where τ_b is the basal shear stress and k and m are constants. The basal shear stress is proportional to the ice thickness, H , times the slope of the ice surface. For simplicity, we assume that the bedrock is flat. After some manipulations, a one-dimensional ice-sheet model based on the conservation of ice mass, can be formulated as follows

$$\frac{\partial H}{\partial t} = \frac{\partial}{\partial x} \left[D \frac{\partial H}{\partial x} \right] + G(x) \tag{2}$$

where

$$D = kH^{m+1} \left| \frac{\partial H}{\partial x} \right|^{m-1}$$

The x axis is oriented in the direction of the mean ice velocity in the drainage system, that is, from the interior of the Antarctic continent to the ocean. The mass balance is denoted by $G(x)$. I have used the model formulated by equation (2) in some other studies. (See ref. 6 for details.) Current values for m are within the 2–3.5 range. Here we adopt a value of 2.5. The flow parameter, k , will be chosen such that the present model produces the correct order of magnitude of ice thickness in a typical Antarctic drainage system.

To make the model more tractable, we will now make it zero-dimensional by inserting in equation (2) typical values of the quantities involved. Let the typical ice thickness be H_0 and the typical horizontal scale for ice thickness variations L_0 . To a first approximation, the dynamics of the drainage system can be described by

$$\frac{dH_0}{dt} = -KH_0^{2m+1}L_0^{-(m+1)} + G_0 \tag{3}$$

The constant, K , is not necessarily the same as k . The steady-state ice thickness can easily be found by setting the dH_0/dt to zero. The resulting relation between H_0 and G_0 is displayed in Fig. 1. L_0 has been set to 1,000 km. Curves are shown for $K = 1, 2$ and $6 m^{-3/2} yr^{-1}$, corresponding to $H_0 = 2,311, 2,055$ and $1,712$ m respectively, for $G_0 = 0.17$ m of ice per yr (which is about the average mass balance of the Antarctic Ice Sheet).

To fit the description of ice-flow dynamics given above into a simple linear stochastic model, equation (3) has to be linearized around some reference state. For this purpose, it is natural to use the present state (although we cannot be sure that at present the Antarctic Ice Sheet is close to equilibrium), which will be

denoted by asterisks. We find

$$\frac{dH'_0}{dt} = -K(2m+1)H_0^{*2m}L_0^{-(m+1)}H'_0 + G'_0 \tag{4}$$

A prime denotes deviation from the reference state. According to equation (4), the relaxation time t_R equals $[K(2m+1)H_0^{*2m}L_0^{-(m+1)}]^{-1}$. Values of t_R corresponding to $H_0^* = 2,353, 2,097$ and $1,746$ m are 2,311, 2,055 and 1,712 yr, respectively. Apparently, t_R is not very sensitive to the particular reference state we choose.

At this point, we interpret $G'_0(t)$ as a stochastic process, representing random fluctuations in the mass balance. The quantity H'_0 is assumed to represent deviations of the mean thickness of the Antarctic Ice Sheet (note that this implies that the various drainage systems have the same dynamical characteristics, which seems a reasonable approximation for this analysis). To keep things as simple as possible, we assume that $G'_0(t)$ is a white-noise process, which implies that the process $H'_0(t)$ has a spectrum proportional to $1/(1+\omega^2 t_R^2)$ (red noise). The total variance of $H'_0(t)$ equals $t_R S_G$, where S_G is the (constant) spectral density of the white noise⁴. In practice, a reliable estimate of S_G is best obtained from mass balance measurements that are averaged over some time. If the averaging time is t , the following relation results:

$$\sigma_{H_0} = (t t_R)^{1/2} \sigma_G \tag{5}$$

Here, σ denotes standard deviation and the tilde indicates that the mass balance is averaged over t yr. Choosing $t_R = 2,100$ yr (intermediate curve in Fig. 1) and $t = 30$ yr, we have $\sigma_{H_0} = 250\sigma_G$.

At this point an estimate of σ_G is needed. Figure 2 shows some proxy data on mass balance variations that were readily available and permit an order-of-magnitude estimate of σ_G . The records are inferred from stratigraphical studies at three locations on the Greenland Ice Sheet⁷ and at the South Pole⁸. The data shown suggest a relative standard deviation for 30-yr mean values of roughly 7%. For the Antarctic Ice Sheet with a mean mass balance of 0.17 m ice per yr, this gives $\sigma_G = 0.012$ m ice yr⁻¹. It cannot be expected that precipitation anomalies are uniform over Antarctica. To correct for this we need to know into how many 'independent' regions Antarctica can be divided. At present, no data are available on the typical horizontal scale of accumulation anomalies over the Antarctic Ice Sheet. We therefore arbitrarily assume that five regions exist where

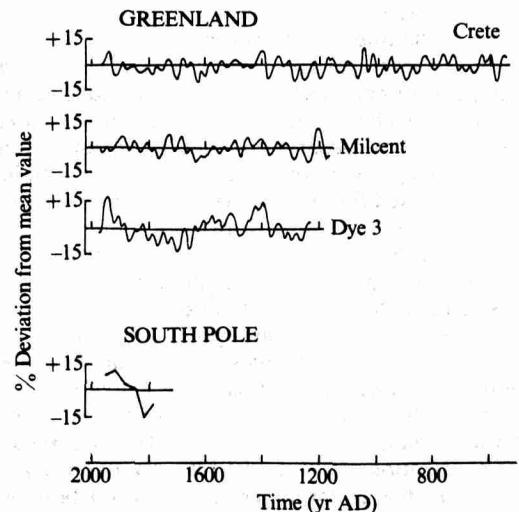


Fig. 2 Time series showing variations in ice accumulation rates, as inferred from stratigraphical studies on the ice of Greenland and Antarctica. The three upper curves are from ref. 7. Variability on time scales smaller than 30 yr has been removed from these curves. The lower curve shows 30-yr mean values of accumulation at the South Pole, computed from data given in ref. 8. Variability is expressed as relative deviation from the mean value.

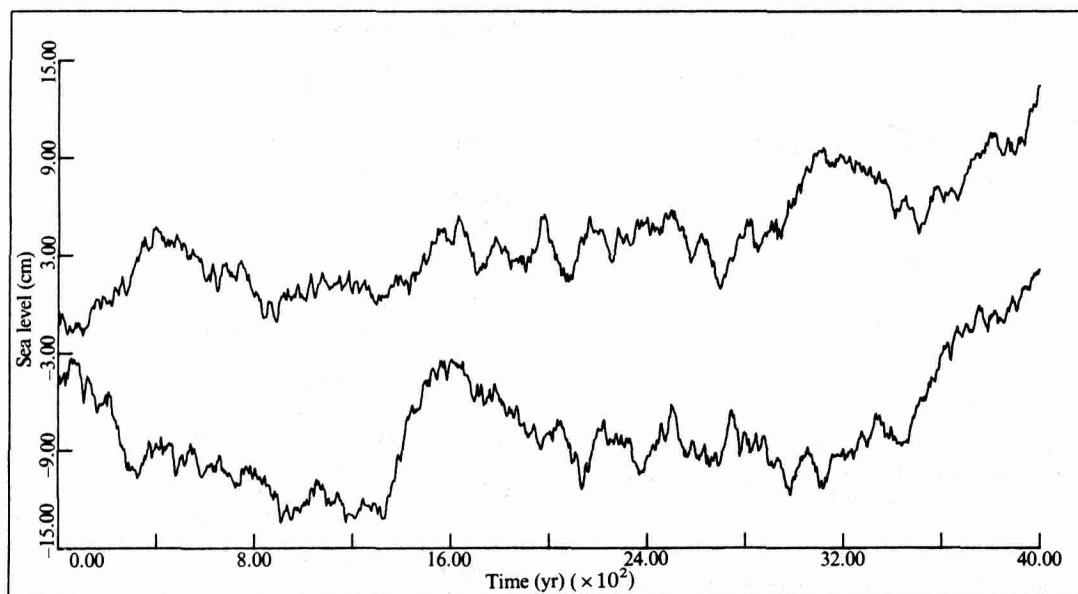


Fig. 3 Two sea-level records generated by the stochastic model, with a length of 4,000 yr. Values of the constants used: $t_R = 2,100$ yr, $\sigma_{\delta} = 0.85$ cm ice per yr.

snowfall fluctuations are uncorrelated. The value of σ_{δ} should then be divided by $\sqrt{5}$, which gives $\sigma_{\delta} = 0.0054$ m ice yr^{-1} . The resulting value of σ_{H_0} is about 1.35 m. As the area of the Antarctic Ice Sheet is $\sim 4\%$ of that of the world ocean, the corresponding standard deviation of the sea level amounts to ~ 5 cm. If we would choose the spatial scale of precipitation much smaller, the value of σ_{H_0} would also be smaller. For example, if nine independent regions were present, σ_{H_0} would be about 1 m.

To show more clearly what happens, Fig. 3 provides two examples of sea-level records generated by equation (4). The process $G'_0(t)$ was simulated by a random number generator, such that $\sigma_{\delta} = 0.008$ m ice yr^{-1} . The records, both spanning, 4,000 yr, show that the major part of the variability is contained in the longer time scales. This is to be expected, because the relaxation time of the ice sheet is of the order of a few thousand years.

The foregoing results clearly demonstrate that stochastic forcing of the Antarctic Ice Sheet by fluctuations in snow accumulation may contribute significantly to variations in global sea level. As revealed in Fig. 3, a sea-level trend of 4 cm in 100 yr can easily be due to the process analysed in this study. Even if local sea-level changes are considered, this is by no means negligible. Other mechanisms creating long-term sea-level variability (like changes in atmospheric wind and pressure patterns, shifts in the oceanic circulation regimes, eustatic effects) lead to changes with the same order of magnitude⁹.

It should be stressed that I have presented here an order-of-magnitude estimate. In the foregoing analysis several uncertainties exist. First, the estimate of σ_{δ} is very crude. A critical survey of all data on accumulation over the Antarctic continent is needed to derive a typical horizontal scale for accumulation anomalies. Another point concerns the very schematic treatment of the dynamics of the Antarctic Ice Sheet. The geometry of Antarctica is rather complicated (large variations in bedrock elevation), so modelling of the ice flow by a zero-dimensional model can only give a crude approximation to reality. The assumption of constant L_0 is a poor approximation for regions where the Antarctic continent is not bounded by deep ocean but by a continental shelf, which makes it possible for the ice sheet to expand horizontally.

In view of these points, perhaps the vertical axis in Fig. 3 should be doubled, or halved. In spite of this uncertainty, however, this study reveals that a substantial part of global sea-level variability may be caused by random forcing of the Antarctic Ice Sheet.

Received 3 December 1980; accepted 18 February 1981.

1. Thomas, R. H., Sanderson, T. J. O. & Rose, K. E. *Nature* **277**, 355–358 (1979).
2. Schwerdtfeger, W. in *World Survey of Climatology* Vol. 14 (ed. Landsberg, H. E.) 253–355 (1970).
3. Giovinetto, M. B. in *Antarctic Snow and Ice Studies*, Antarctic Res. Ser. 2 (ed. Mellor, M.) 127–155 (American Geophysical Union, 1964).
4. Hasselmann, K. *Tellus* **28**, 473–485 (1976).
5. Nye, J. F. *J. Glaciol.* **3**, 493–507 (1959).
6. Oerlemans, J. *Tellus* **33**, 1–12 (1981).
7. Reeh, N. *et al. J. Glaciol.* **20**, 27–30 (1978).
8. Giovinetto, M. B. & Schwerdtfeger, W. *Arch. Meteorol. Geophys. Bioklimatol.*, Ser. A **15**, 228–250 (1966).
9. Lisitzin, E. *Sea-level Changes* (Elsevier, Amsterdam, 1974).

The Caledonian nappes of eastern North Greenland

John Malcolm Hurst* & William Stuart McKerrow†

* Grønlands Geologiske Undersøgelse, Øster Voldgade 10, 1350 Copenhagen K, Denmark

† Department of Geology and Mineralogy, Parks Road, Oxford OX1 3PR, UK

Reconnaissance work in Kronprins Christian Land^{1–7} indicated the presence of one main nappe of late Proterozoic sediments^{2,3} thrust over Lower Palaeozoic platform carbonates similar to Peary Land^{7,8}. Our 2-month helicopter-supported work in 1980 now indicates the presence of three thrust-bounded nappes. The Finderup Land Nappes, which occur in northern Kronprins Christian Land, contain a late Precambrian early Cambrian sequence in thrust contact above Silurian carbonates. The younger Vandredalen Nappe in thrust contact above the Finderup Land Nappes and Silurian carbonates occurs throughout Kronprins Christian Land and contains a thick sequence of late Proterozoic clastics and carbonates. In southern Kronprins Christian Land the Sæfaxi Elv Nappe only contains Ordovician–?Silurian carbonates and is in thrust contact below Vandredalen Nappe. The nappes were involved in westward-directed thrusting (>150 km) and are probably a result of continental collision when the northern part of Iapetus Ocean closed in the late Silurian.

On the east coast of Kronprins Christian Land (Fig. 1), a narrow belt of gneisses crops out to the east of Proterozoic sandstones which have been referred previously to the Thule Group^{5,6,9}. Both are probably equivalent to the Proterozoic Independence Fjord Group west of Danmark Fjord¹⁰ (Fig. 1).